Age-dependent dissociation of ATP synthase dimers and loss of inner-membrane cristae in mitochondria

Bertram Daum[a], Andreas Walter[a], Angelika Horst[a], Heinz D. Osiewacz[b,c], and Werner Kühlbrandt[a,c,1]

[a]Department of Structural Biology, Max Planck Institute of Biophysics, 60438 Frankfurt am Main, Germany; [b]Molecular Developmental Biology, Goethe University, 60438 Frankfurt am Main, Germany; and [c]Cluster of Excellence Frankfurt "Macromolecular Complexes," Deutsche Forschungsgemeinschaft, 60438 Frankfurt am Main, Germany

Edited by Richard Henderson, Medical Research Council Laboratory of Molecular Biology, Cambridge, United Kingdom, and approved July 22, 2013 (received for review April 3, 2013)

Aging is one of the most fundamental, yet least understood biological processes that affect all forms of eukaryotic life. Mitochondria are intimately involved in aging, but the underlying molecular mechanisms are largely unknown. Electron cryotomography of whole mitochondria from the aging model organism *Podospora anserina* revealed profound age-dependent changes in membrane architecture. With increasing age, the typical cristae disappear and the inner membrane vesiculates. The ATP synthase dimers that form rows at the cristae tips dissociate into monomers in inner-membrane vesicles, and the membrane curvature at the ATP synthase inverts. Dissociation of the ATP synthase dimer may involve the peptidyl prolyl isomerase cyclophilin D. Finally, the outer membrane ruptures near large contact-site complexes, releasing apoptogens into the cytoplasm. Inner-membrane vesiculation and dissociation of ATP synthase dimers would impair the ability of mitochondria to supply the cell with sufficient ATP to maintain essential cellular functions.

subtomogram averaging | cell death

Mitochondria are semiautonomous organelles with an outer and an inner membrane, dedicated to ATP production in all eukaryotes. The inner mitochondrial membrane is highly folded into cristae (1–3), which contain the bulk of the respiratory chain complexes and the mitochondrial F_1F_o ATP synthase (4, 5). At the cristae ridges, the ATP synthase self-assembles into long rows of dimers, which maintain a high local membrane curvature and normal cristae architecture (1, 6, 7). Respiratory chain complexes at either side of the dimer rows (1) pump protons from the mitochondrial matrix into the cristae space. The resulting protonmotive force drives the production of ATP.

Mitochondria are implicated in aging and cell death in several ways. In the course of electron-transfer reactions, complexes I and III generate superoxide radicals (8), which inflict oxidative damage on mitochondria and other cellular components. Cells normally deal with this type of damage with various responses, including a combination of mitochondrial fission and fusion. Damaged or dysfunctional mitochondria are either complemented with a healthy part of the mitochondrial network by fusion or sorted out for mitophagy (9). The equilibrium between fusion and fission normally maintains a reticulate mitochondrial network (9, 10). During aging, fission overpowers fusion and the mitochondrial network fragments (11). This prevents complementation of damaged mitochondria by fusion and thus accelerates their deterioration.

Cumulative oxidative damage promotes cellular and organismal senescence (12). It can cause neurodegeneration (13), and ultimately results in programmed cell death (14, 15). Programmed cell death is triggered by the release of apoptogens, such as cytochrome *c* (cyt-*c*), through pores that open in the outer mitochondrial membrane (16). Cyt-*c* activates a cascade of proteolytic caspases, which degrade cellular proteins indiscriminately. Two distinct pore types have been postulated: the mitochondrial permeability transition pore complex (mPTPC) (17) and the mitochondrial apoptosis-induced channel (16), which is thought to occur mainly in vertebrates (18). In response to adenine nucleotide depletion, calcium, or oxygen radicals (19, 20), the mPTPC is thought to form in the inner mitochondrial membrane upon binding of cyclophilin D (CypD) on the matrix side. According to current models (16), a small inner-membrane pore initially results in the influx of water, ions, and small molecules. The mitochondria swell and the outer membrane ruptures, releasing apoptogens (17, 21). The exact protein composition of the putative mPTPC and its mode of action are unknown (16, 19).

With a short, defined life span of 15–20 d and a fully sequenced genome (10), the wild-type "s" strain of *P. anserina* is an excellent model to investigate the causes and effects of aging at the organellar and molecular level. *P. anserina* shares many age-related phenomena with mammals, including the generation or scavenging of oxygen radicals, instability of mitochondrial DNA, and the role of protein quality control in aging (10). In *P. anserina* and yeast knockout mutants lacking the mitochondrial dynamin-like protein Dnm1 that promotes fission, fragmentation of the mitochondrial network is delayed, which in *P. anserina* results in a ninefold longer life span (11). Conversely, yeast strains lacking the dynamin-like fusion protein Mgm1 [mitochondrial genome maintenance 1; corresponding to OPA1 (optic atrophy 1) in mammals] are incapable of mitochondrial fusion and have a reduced replicative and chronological life span (22).

In an earlier electron cryotomography (cryo-ET) study (23), we found that *P. anserina* mitochondria undergo a major morphological change during senescence, whereby the inner membrane fragments into vesicles. Because cristae formation depends on assembly of the ATP synthase dimers into rows (6), we asked whether we could detect any age-dependent changes of this arrangement.

Overexpression of the gene encoding the mPTPC component CypD accelerated inner-membrane fragmentation and senescence by a factor of 3 (23), suggesting that mitochondrial permeability transition plays a fundamental role in aging. *P. anserina* cultures have been found to die by mPTP-induced apoptosis (24), and the mPTPC also seems to be involved in mammalian aging. Mitochondria in the brain of aged rodents are more sensitive to Ca^{2+}-induced permeability transition compared with the young mature rodent brain (25).

Here we report a series of profound changes of membrane structure and macromolecular organization in mitochondria of aging *P. anserina*. The changes include the retraction of cristae

Author contributions: B.D. and W.K. designed research; B.D., A.W., and A.H. performed research; H.D.O. contributed new reagents/analytic tools; H.D.O. provided *Podospora* cultures; B.D. analyzed data; and B.D. and W.K. wrote the paper.

The authors declare no conflict of interest.

This article is a PNAS Direct Submission.

Freely available online through the PNAS open access option.

[1]To whom correspondence should be addressed. E-mail: werner.kuehlbrandt@biophys.mpg.de.

This article contains supporting information online at www.pnas.org/lookup/suppl/doi:10.1073/pnas.1305462110/-/DCSupplemental.

CELL BIOLOGY

lamellae into the inner boundary membrane, fragmentation of the mitochondrial matrix, and disassembly of ATP synthase dimer ribbons into monomers. Finally, the inner-membrane vesicles swell and the outer membrane ruptures. These changes would have a major impact on the energy supply and cellular fitness in the senescent organism.

Results and Discussion

The Mitochondrial Inner Membrane Vesiculates with Age. We performed cryo-ET on mitochondria isolated from young (6 d), middle-aged (9 d), or senescent (15 d or older) *P. anserina*. In young cultures, 63% of the mitochondria had well-separated lamellar cristae projecting 400 nm or more into a single, continuous matrix (Fig. 1*A*). This is the typical, standard mitochondrial morphology. In the remaining 37% of mitochondria, the matrix had broken up into a number of separate, irregular vesicles. The fraction of mitochondria with vesicular morphology increased to 48% in middle-aged and to 86% in senescent cultures (Fig. 1 *B–D*), indicating a substantial shift from the standard morphology to the vesicular morphology within the *P. anserina* life span. We did not observe matrix vesiculation in mitochondria from a range of other organisms that do not undergo synchronized aging (1). Therefore, the observed changes were not due to the isolation procedure.

Closer inspection revealed three different types of vesicular mitochondria. The morphology we refer to as "partly lamellar" (Fig. 1*B*) was often found in middle-aged cultures. In these mitochondria, the inner membrane formed a small number of large (>350 nm) vesicles with short lamellar cristae. The remainder of the inner membrane was fragmented into separate <350-nm vesicles, which lacked cristae entirely. With increasing age, the fragmentation of the inner membrane progressed to a morphology we refer to as "early-vesicular" (Fig. 1*C*). As before, vesicles of different shapes and sizes were contained within the outer membrane, but none of them had cristae. Instead, there were shallow ridges that extended ~20 nm into the matrix. The gap between the outer membrane and the inner boundary membrane had widened from typically 12 ± 2.5 nm to 40 nm or more. Finally, in senescent cultures, the morphology we refer to as "late-vesicular" predominated (Fig. 1*D*). The fragmentation into irregular or spherical vesicles was complete. Vesicles were rarely larger than ~200 nm and the membrane curvature was almost entirely concave.

Age-dependent vesiculation of the inner membrane is most likely due to accumulating oxidative damage. When the number of dysfunctional mitochondria in aging organisms passes a certain threshold, the cellular surveillance and repair processes fail and programmed cell death ensues (9, 26). In *P. anserina* and similar organisms with short life cycles that spend most of their available energy on reproduction, mechanisms of mitochondrial maintenance, such as fission and fusion, may be less well developed than in longer-lived multicellular organisms. Alternatively,

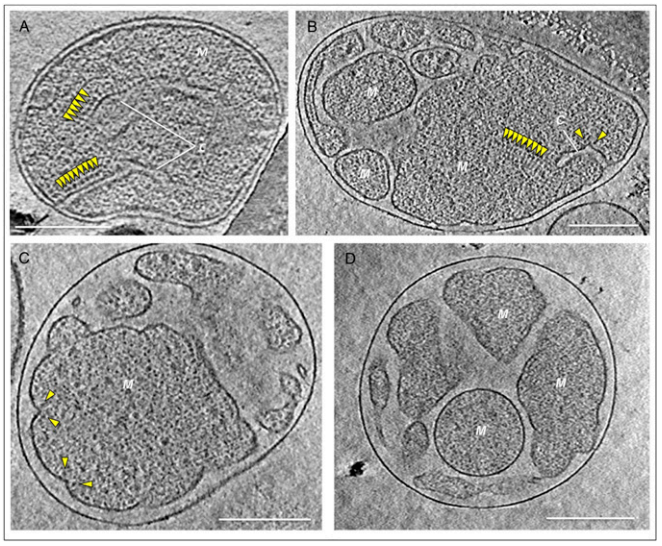

Fig. 1. Age-dependent morphology changes in *P. anserina* mitochondria. (*A*) Mitochondria of standard morphology, typical for young (6-d-old) *P. anserina*, have lamellar cristae studded with ATP synthase dimer rows visible in cross-section (yellow arrowheads). The distance between the inner and outer membranes is ~12 nm. (*B–D*) Mitochondrial morphologies typical for senescent *P. anserina* cultures. (*B*) In partly lamellar mitochondria, the inner membrane begins to break up into vesicles. Only vesicles >350 nm contain cristae and ATP synthase dimer rows (yellow arrowheads). (*C*) In the early-vesicular morphology, shallow membrane ridges carry ATP synthase dimers (yellow arrowheads). The cristae junctions and intermembrane space have widened to ~40 nm. (*D*) In the late-vesicular morphology, the curvature of the inner membrane is mostly concave without cristae ridges or ATP synthase dimers. C, cristae; M, matrix. (Scale bars, 200 nm.) Mitochondria were isolated from 6-d-old (*A*), 9-d-old (*B*), and ~15-d-old cultures (*C* and *D*).

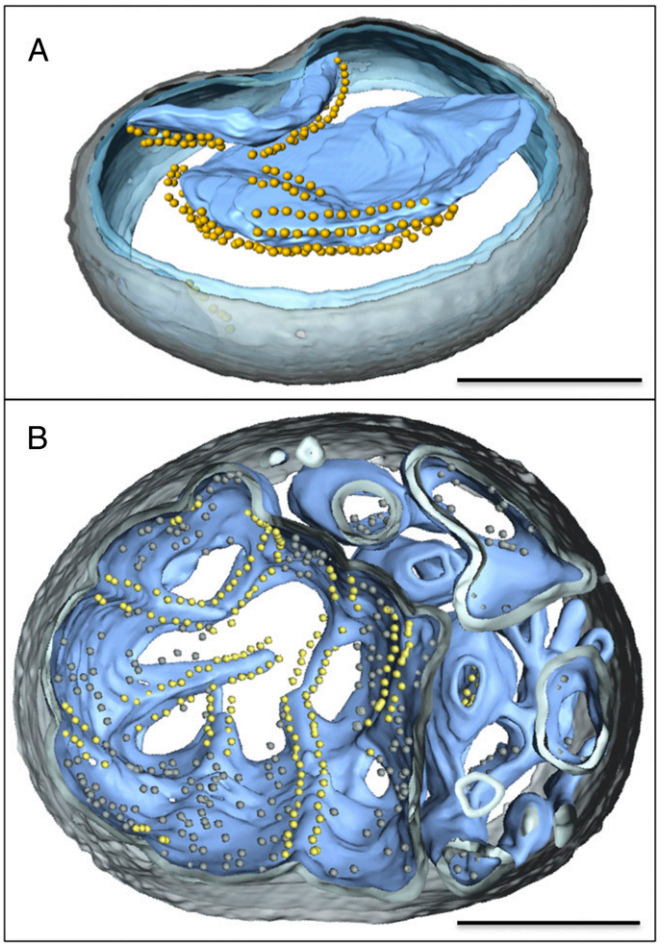

Fig. 2. Three-dimensional tomographic volumes of mitochondria with standard or early-vesicular morphology. Segmented tomographic volume of mitochondria with standard (*A*) and early-vesicular morphology (*B*). In *A*, the ATP synthase dimers are arranged in rows along highly curved apices of inner-membrane cristae. In *B*, ATP synthases dimer rows are arranged along shallow inner-membrane ridges in matrix compartments with diameters >350 nm. Smaller inner-membrane vesicles show no evidence of ATP synthase dimers or dimer rows. Outer membrane, transparent gray; inner membrane, transparent blue; cristae, light blue. ATP synthase F_1 heads are shown as yellow spheres. (Scale bars, 200 nm.)

a short life span may be genetically programmed so that long-lived individuals and their offspring do not compete for the same resources (27).

Membrane remodeling resembling inner-membrane vesiculation in aging *P. anserina* has been observed in mitochondria during induced apoptosis, such as in etoposide-treated HeLa cells (28, 29) or in isolated mouse mitochondria after addition of the pro-apoptotic protein tBID (truncated BH3 interacting domain death agonist) (30). Similar changes in inner-membrane organization have been found to occur in at least 25 different disease conditions, including severe neurodegenerative diseases (31). These changes have so far not been investigated at the level of membrane organization or macromolecular structure. Vesiculation of the inner membrane has been found to result in a loss of mitochondrial membrane potential (29) and strongly reduced respiratory activity (32). Aging cells in which the inner membrane vesiculates are likely to be affected in the same way.

ATP Synthase Dimers Dissociate in Aged Mitochondria. Because cristae formation depends on assembly of the ATP synthase into dimer rows (6), we asked whether there were any age-dependent changes in molecular organization of the inner membrane, in particular of the ATP synthase. Mitochondria from juvenile cultures with standard morphology showed numerous 11-nm particles arranged in pairs that formed long rows along the highly curved cristae tips (Figs. 1*A* and 2*A*). Each particle was connected to the membrane by a 4-nm stalk. Subtomogram averaging of the same particle pairs in yeast (6) and other organisms (1) has shown that they are dimers of the mitochondrial ATP synthase. Dimer rows were always present along the highly curved cristae tips in the partly lamellar morphology (Fig. 1*B*) and along shallow membrane ridges in early-vesicular mitochondria (Figs. 1*C* and 2*B*; Movie S1). Dimer rows were found only in large, >350-nm vesicles. No dimers were evident in the smaller (200- to 350-nm) vesicles at the partly lamellar or early-vesicular stage (Fig. 1 *B* and *C*). Instead, these vesicles contained numerous monomeric 11-nm particles. Late-vesicular mitochondria, where the entire matrix was fragmented into smaller vesicles, completely lacked dimer rows (Fig. 1*D*).

Distances between particles protruding 15 nm from cristae tips in the standard morphology (Fig. 3 *A* and *B*) or matrix vesicles from the late-vesicular morphology (Fig. 3 *D* and *E*) were analyzed by weighted histograms (Fig. 3 *C* and *F*). Particles protruding about 15 nm into matrix vesicles were either ATP synthase monomers or the matrix arm of complex I, the only known complexes of this size in the inner membrane. In mitochondria, the ATP synthase outnumbers complex I by 3.6 to 1 (1). The histograms are therefore dominated by distances between the ATP synthase F_1 heads in the membrane.

The four peaks in the histogram of standard, juvenile mitochondria (Fig. 3*C*) indicate the most frequently observed interparticle distances. The first peak at around 17 (±2) nm is the average nearest-neighbor distance between two ATP synthase F_1 heads along the dimer rows (Fig. 4*B*). The peaks at 35 (±2) nm and 50 (±2) nm are multiples of this distance by a factor of 2 or 3. The peak at 30 (±2) nm corresponds to the distance between the two F_1 heads within the ATP synthase dimer (Fig. 4*B*) (1, 6, 33).

The histogram of late-vesicular, senescent mitochondria (Fig. 3*F*) shows no peaks at these distances. Instead, there is a roughly even distribution of interparticle distances beyond a single broad maximum at ∼14 nm, the average closest distance between two monomeric ATP synthases in the membrane. The absence of peaks in the 17- to 50-nm range indicates that matrix vesicles from senescent *P. anserina* do not contain detectable numbers of ATP synthase dimers. We conclude that the dimer rows disperse and the ATP synthase dimers dissociate into monomers with increasing age.

We have shown previously that the formation of inner-membrane cristae depends on the presence of ATP synthase dimers (6). Computer simulations indicate that the dimers induce membrane curvature, and not that, conversely, membrane curvature induces dimer formation (6). Yeast mutants in which the dimer-specific ATP synthase subunits *e* or *g* were knocked out lacked ATP synthase dimers, dimer rows, and lamellar cristae. In these mutants, the membrane potential is reduced by 40–70% (34), the respiration rate drops by up to 50%, and the generation time increases by about 50% (7, 34). This indicates that the ATP synthase dimer rows are necessary for the formation of the inner-membrane cristae. Aging in *P. anserina* is thus at least in part the result of an insufficient energy supply to the cell, due to inner-membrane vesiculation that would render the mitochondria unable to produce sufficient ATP to maintain vital cellular functions.

The Structure of the ATP Synthase Dimer Changes in Aging Mitochondria. To find out whether and how the structure of the ATP synthase itself changes during aging, we examined young, middle-aged, and senescent mitochondria by subtomogram averaging (Fig. 4). The averaged volume from juvenile samples shows two ATP synthase monomers forming a V-shaped dimer in the membrane (Fig. 4*A*),

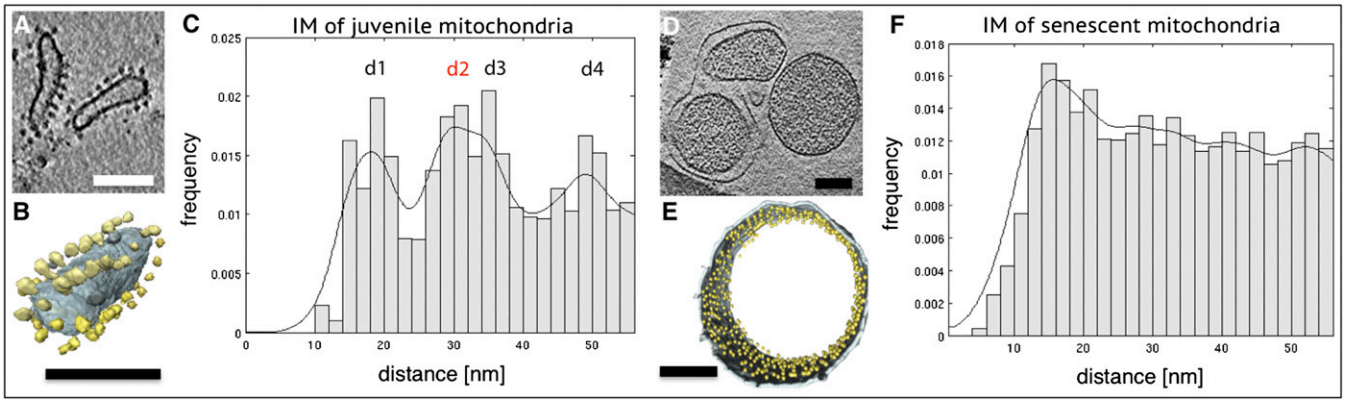

Fig. 3. Age-dependent changes of the mitochondrial ATP synthase. (*A* and *B*) Tomographic slice (*A*) and segmented subvolume (*B*) of cristae vesicles from a 6-d-old mitochondrion with standard morphology. ATP synthase dimer rows (yellow) project from the inner membrane. (*C*) Histogram of distances between particles projecting from the cristae vesicles shown in *A* or *B*. Peaks d1, d3, and d4 correspond to multiples of the average distance between two consecutive dimers within a row. Peak d2 indicates the distance between the two F_1 heads in a dimer. IM, inner membrane. (*D* and *E*) Tomographic slice (*D*) and segmented subvolume (*E*) of a matrix vesicle isolated from a fully vesicular mitochondrion. ATP synthase monomers (yellow) project from the membrane into the interior of the vesicle without long- or short-range order. (*F*) Histogram of distances between all ATP synthase-like particles in *D* and *E*. (Scale bars, 100 nm.)

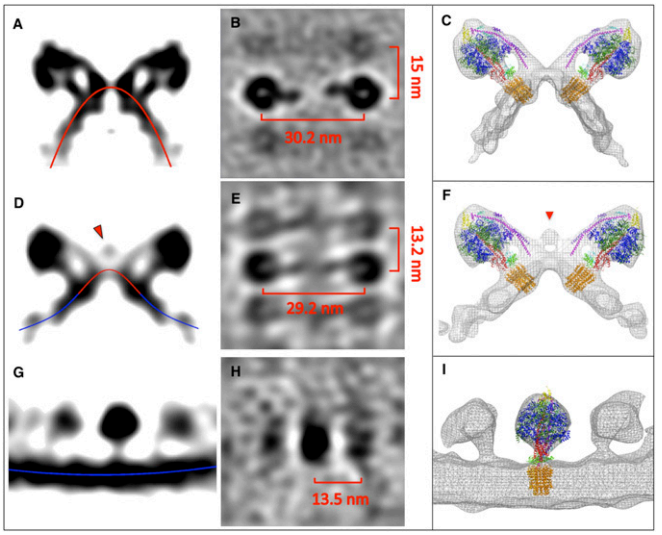

Fig. 4. Age-dependent changes in ATP synthase structure. (*A* and *B*) Side (*A*) and top view (*B*) of subtomogram-averaged ATP synthase dimer from 6-d-old *P. anserina* mitochondria with standard morphology. (*D* and *E*) Subtomogram-averaged ATP synthase dimer from shallow membrane ridges of early-vesicular mitochondria. (*G* and *H*) ATP synthase monomer from an inner-membrane vesicle of late-vesicular mitochondria. (*C*, *F*, and *I*) Subtomogram averages with fitted X-ray models (6). Red lines indicate convex membrane curvature (as seen from the matrix); blue lines indicate concave membrane curvature. Red arrowheads mark a density connecting the peripheral stalks in ATP synthase dimers from early-vesicular mitochondria.

with a center-to-center distance between the F_1 heads of ~30 nm (Fig. 4*B*). Rigid-body superposition of the yeast dimer model (6) on the *P. anserina* volume resulted in a perfect fit, indicating that the two dimers were virtually identical (Fig. 4*C*). As in yeast, the peripheral and central stalks of the ATP synthase were well-resolved (Fig. 4*A*), indicating a comparable resolution of ~4 nm. The subtomogram average shows the neighboring ATP synthase dimers in the row as fainter, blurred densities at a distance of ~15 nm (Fig. 4*B*), consistent with the slightly irregular dimer spacing along the row (6). In cross-section, the membrane describes a sharply curved convex arc (red line in Fig. 4*A*), with the apex at the twofold symmetry axis.

Next, we aligned and averaged ATP synthase dimers from the shallow membrane ridges of early-vesicular mitochondria (Fig. 4 *D* and *E*). Again, the yeast atomic model fitted the map closely (Fig. 4*F*). However, in cross-section, the membrane now described a shallow bell-shaped curve, with a convex apex between the F_o rotor rings (red in Fig. 4*D*), gradually changing to concave curvature at either side (blue in Fig. 4*D*). Strikingly, the dimer volume indicated an additional density bridging the two peripheral stalks (Fig. 4 *D* and *F*), which was absent in the averages of ATP synthase dimers from young cultures. The extra density was found in independent subtomogram averages from different mitochondria at the same stage of aging. It was also found in individual unsymmetrized dimers (Fig. S1 *A*–*D*) and in consecutive dimers within a row (Fig. S1 *C*, *D*, and *F*), indicating that it was not due to random noise. It is most likely a matrix protein that interacts with the ATP synthase dimer before the dimers finally dissociate. This protein may be a factor acting on the ATP synthase subunits that are required for the formation of ATP synthase dimers (35), dimer rows (1), and regular cristae (6, 7).

It has been found that overexpression of the gene encoding the mPTPC component CypD in *P. anserina* induces inner-membrane vesiculation and accelerates aging (23). Giorgio et al. (36) reported that CypD association with the peripheral stalk modulates ATP synthase activity. Together, these observations suggest that the extra density in Fig. 4 *D* and *E* may be CypD. We fitted an atomic model of the C-terminal domain of *P. anserina* CypD (residues 41–166) based on the human crystal structure (Protein Data Bank ID code 2bit) to this part of the map volume (Fig. S2 *A* and *B*). The fit places CypD close to regions of the peripheral stalk that are likely to contain the N-terminal part of subunit *b* (Fig. S2 *A* and *B*, magenta) (37, 38), for which there is at present no X-ray structure. However, more recently, Giorgio et al. reported that CypD interacts with the ATP synthase subunit OSCP (39), which is located on top of the F_1 head (Fig. S2 *A* and *B*, yellow), and that this causes the ATP synthase dimer to form the mPTPC. Further investigation by electron tomography and biochemistry is required to resolve this issue.

It is conceivable that the peptidyl prolyl isomerase CypD binds to subunit *b* as well as OSCP, which both contain conserved proline residues (Fig. S3). CypD might isomerize proline peptide bonds in these proteins, which could result in conformational changes. The N terminus of subunit *b* is known to stabilize the ATP synthase dimer (40). *cis–trans* isomerization of prolyl bonds by CypD may thus promote the dissociation of the dimers as a prerequisite for complete inner-membrane vesiculation.

Inner-Membrane Vesicles in Senescent Mitochondria Contain ATP Synthase Monomers and Large Contact-Site Complexes. Finally, we averaged the 11-nm particles projecting into the inner-membrane

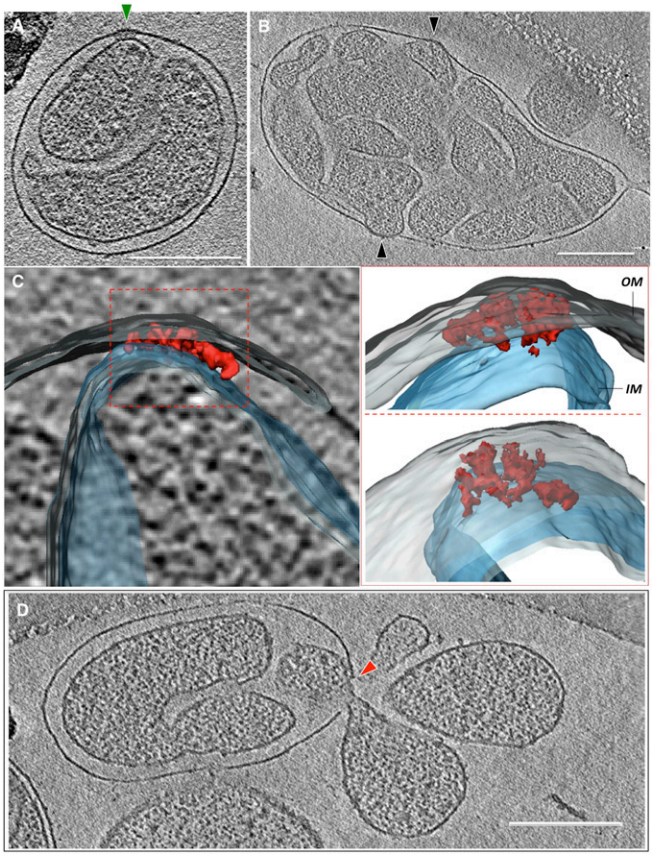

Fig. 5. Contact sites in senescent mitochondria. (*A*) An ~45-nm protein complex at a contact site between the inner and outer membranes (green arrowhead). (*B*) Membrane contact sites (black arrowheads). (*C*) Three different views of the segmented, surface-rendered subtomogram of the contact site shown in *A*. The contact-site complex (red) consists of several discrete densities spanning the inner (transparent blue) and outer membranes (OM) (transparent gray). (*D*) Ruptures in the outer membrane (red arrowhead) frequently develop next to contact-site complexes. (Scale bars, 200 nm.)

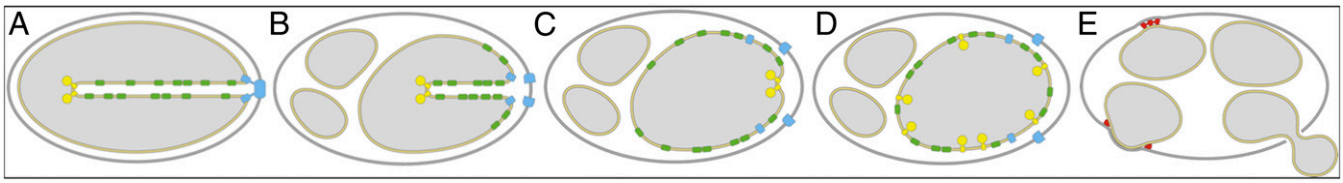

Fig. 6. Model of age-dependent membrane reorganization in mitochondria. (*A*) In the standard morphology, the inner-membrane cristae carry rows of ATP synthase dimers (yellow) at the apex. For simplicity, the dimer row is drawn in cross-section through one ATP synthase dimer. Respiratory chain complexes (green) occupy the membrane regions at either side. The membrane turns sharply into the matrix at the cristae junction complex (blue). (*B*) At an early stage of mitochondrial aging, the inner membrane partly vesiculates and the cristae recede, which requires the cristae junction complex to disassemble. (*C*) At the next stage, the inner membrane forms shallow ridges carrying rows of ATP synthase dimers. The cristae junction complex no longer maintains a sharp membrane bend. (*D*) At the final aging stage, the cristae have disappeared completely and the inner membrane is fully vesicular. The ATP synthase dimers dissociate into monomers and the membrane curvature with respect to the ATP synthase is concave. The previously segregated membrane protein complexes of the cristae and the inner boundary membrane are intermixed. (*E*) Finally, the inner-membrane vesicles swell and attach to the outer membrane near large contact-site complexes. Eventually the outer membrane ruptures, releasing matrix vesicles and cyt-*c* into the cytoplasm.

vesicles at the late-vesicular stage (Figs. 1*D* and 3 *D* and *E*). The resulting volume had the shape and dimensions of the ATP synthase (Fig. 4*G*) and matched the atomic model of a single ATP synthase monomer (6) (Fig. 4*I*). At either side, two fainter densities appeared at a distance of 13.5 ± 2 nm, similar to the closest interparticle spacing indicated by the corresponding histogram (Fig. 3*F*). Note that there were no F_1 densities at a distance of 28–30 nm, characteristic of ATP synthase dimers. The peripheral stalk was not visible, due to the random orientation of the ATP synthase monomers in the membrane. The bilayer was concave (Fig. 4*G*, blue), with no sign of the local convex membrane curvature associated with the ATP synthase dimer rows.

Late-vesicular mitochondria frequently displayed several sites of close contact between the inner and outer membranes, covering areas up to ∼6,000 nm^2 (Fig. 5*B* and Movie S2). At these membrane contact sites, the inner and outer membranes both bulged outward (Fig. 5*B* and Movies S2 and S3). The membranes were closely appressed and no aqueous intermembrane space was resolved (Fig. 5*B* and Movies S2 and S3). Adjacent to these appressed membrane regions, large assemblies of membrane proteins spanning the inner and outer membranes were occasionally observed (Fig. 5*A* and Movies S3, S4, and S5). Manual segmentation revealed that these assemblies consisted of several similar-sized parts (Fig. 5*C*). Overall, the complexes were roughly disk-shaped, with diameters up to 45 nm and a thickness of ∼20 nm, including both membranes (Fig. 5 *A* and *B* and Movie S5. Their approximate molecular mass, estimated from their dimensions, was in the range of 10–20 MDa. Usually, only one of these large double-membrane–spanning assemblies was found per mitochondrion. Occasionally, matrix vesicles were seen to escape into the surrounding medium at breaks in the outer membrane near these sites (Fig. 5*D*).

Apoptosis is widely assumed to involve the mPTPC (17), which opens a small inner-membrane pore that leads to the influx of water, ions, and small molecules (16), causing the mitochondrial matrix to swell and the outer membrane to rupture (17, 21). It has been postulated that the mPTPC forms at contact sites between the inner and outer mitochondrial membranes (41). The extensive contacts between the inner and outer membranes we observe at the final stage of inner-membrane vesiculation in *P. anserina* may be these sites. Membrane rupture in the vicinity of these sites would result in a sudden release of apoptogenic cyt-*c* into the cytoplasm, which in turn would trigger programmed cell death as the final step in cellular senescence.

Conclusion

Electron cryotomography of mitochondria isolated from aging *P. anserina* revealed a sequence of events that includes progressive vesiculation of the mitochondrial inner membrane, collapse of the cristae, disassembly of ATP synthase dimers, and formation of large contact sites between the inner and outer mitochondrial membranes, as summarized in Fig. 6.

Initially, in normal mitochondria of young cells, the cristae protrude deep into the matrix (Fig. 6*A*). The cristae contain the respiratory chain complexes and the mitochondrial F_1F_o ATP synthase (4, 5). Whereas the ATP synthase is located at the highly curved cristae ridges, respiratory chain complexes reside in the membrane regions at either side (1). Cristae formation depends both on the rows of ATP synthase dimers at the tips or ridges and on a complex at the cristae junctions (42–44). This cristae junction complex presumably prevents the diffusion of proteins from the cristae into the boundary membrane and anchors the inner membrane locally to the outer membrane. This complex has to come apart to enable the cristae to collapse and the intermembrane space to widen (Fig. 6*B*). At this stage, the inner membrane begins to break up into vesicles within the outer membrane. As the cristae shorten and collapse, the respiratory chain complexes are pushed into the inner boundary membrane and thus previously segregated protein populations of the inner membrane become intermixed (Fig. 6*C*). Eventually, the cristae disappear completely and the protein composition of the inner membrane is randomized (Fig. 6*D*). At the final stage of mitochondrial senescence, the outer membrane ruptures near, these contact sites. As a result, inner membrane vesicles, along with the apoptogenic cytochrome *c*, escape into the cytoplasm (Fig. 6*E*).

The lateral segregation of respiratory chain complexes and the membrane curvature induced by the ATP synthase dimers at the cristae tips in normal mitochondria are thought to be important for effective ATP synthesis under physiological conditions (1, 33). The disruption of this arrangement would impair the ability of mitochondria to produce ATP at a rate sufficient to keep the organism healthy and competitive. Mitochondria of the senescent, vesicular morphology that lack cristae and ATP synthase dimers cannot maintain a sufficient supply of ATP to the cell. Aging cells with an increasing proportion of dysfunctional mitochondria are less fit and eventually die.

Methods

Mitochondria were isolated from young (6-d), middle-aged (9-d), or senescent (15-d or older) individual *P. anserina* cultures and prepared for electron cryotomography. Tomographic tilt series were recorded using an FEI Polara transmission electron microscope equipped with a postcolumn energy filter, reconstructed into tomographic volumes with IMOD (45), and segmented using the program AMIRA (Mercury Systems). Subtomogram averaging was performed with IMOD (45) and PEET (46). Atomic models were fitted with UCSF Chimera (47). Distances between particles projecting from inner mitochondrial membranes as well as membrane curvature were analyzed by MATLAB (MathWorks). See *SI Methods* for details.

ACKNOWLEDGMENTS. We thank Alexandra Werner for preparation of mitochondria from age-matched *Podospora anserina* cultures, Paolo Lastrico for drawing Fig. 6, Karen Davies, Sebastian Daum, and Vicki Gold for discussion,

CELL BIOLOGY

and Deryck Mills for maintenance of electron microscopes. This work was supported by the Max Planck Society (B.D., A.W., A.H., and W.K.), the Deutsche Forschungsgemeinschaft (H.D.O.; Os75/12-1,2), and the Cluster of Excellence Frankfurt "Macromolecular Complexes" (H.D.O. and W.K.).

1. Davies KM, et al. (2011) Macromolecular organization of ATP synthase and complex I in whole mitochondria. *Proc Natl Acad Sci USA* 108(34):14121–14126.
2. Frey TG, Renken CW, Perkins GA (2002) Insight into mitochondrial structure and function from electron tomography. *Biochim Biophys Acta* 1555(1–3):196–203.
3. Mannella CA, et al. (2001) Topology of the mitochondrial inner membrane: Dynamics and bioenergetic implications. *IUBMB Life* 52(3–5):93–100.
4. Gilkerson RW, Selker JM, Capaldi RA (2003) The cristal membrane of mitochondria is the principal site of oxidative phosphorylation. *FEBS Lett* 546(2–3):355–358.
5. Vogel F, Bornhövd C, Neupert W, Reichert AS (2006) Dynamic subcompartmentalization of the mitochondrial inner membrane. *J Cell Biol* 175(2):237–247.
6. Davies KM, Anselmi C, Wittig I, Faraldo-Gómez JD, Kühlbrandt W (2012) Structure of the yeast F_1F_o-ATP synthase dimer and its role in shaping the mitochondrial cristae. *Proc Natl Acad Sci USA* 109(34):13602–13607.
7. Paumard P, et al. (2002) The ATP synthase is involved in generating mitochondrial cristae morphology. *EMBO J* 21(3):221–230.
8. Dröse S, Brandt U (2012) Molecular mechanisms of superoxide production by the mitochondrial respiratory chain. *Adv Exp Med Biol* 748:145–169.
9. Twig G, Shirihai OS (2011) The interplay between mitochondrial dynamics and mitophagy. *Antioxid Redox Signal* 14(10):1939–1951.
10. Scheckhuber CQ, Osiewacz HD (2008) *Podospora anserina*: A model organism to study mechanisms of healthy ageing. *Mol Genet Genomics* 280(5):365–374.
11. Scheckhuber CQ, et al. (2007) Reducing mitochondrial fission results in increased life span and fitness of two fungal ageing models. *Nat Cell Biol* 9(1):99–105.
12. Navarro A, Boveris A (2007) The mitochondrial energy transduction system and the aging process. *Am J Physiol Cell Physiol* 292(2):C670–C686.
13. Muller FL, Lustgarten MS, Jang Y, Richardson A, Van Remmen H (2007) Trends in oxidative aging theories. *Free Radic Biol Med* 43(4):477–503.
14. Wallace DC (2011) Bioenergetic origins of complexity and disease. *Cold Spring Harb Symp Quant Biol* 76:1–16.
15. Farrugia G, Balzan R (2012) Oxidative stress and programmed cell death in yeast. *Front Oncol* 2:64.
16. Kinnally KW, Peixoto PM, Ryu SY, Dejean LM (2011) Is mPTP the gatekeeper for necrosis, apoptosis, or both? *Biochim Biophys Acta* 1813(4):616–622.
17. Kroemer G, Galluzzi L, Brenner C (2007) Mitochondrial membrane permeabilization in cell death. *Physiol Rev* 87(1):99–163.
18. Bender CE, et al. (2012) Mitochondrial pathway of apoptosis is ancestral in metazoans. *Proc Natl Acad Sci USA* 109(13):4904–4909.
19. Halestrap AP (2009) What is the mitochondrial permeability transition pore? *J Mol Cell Cardiol* 46(6):821–831.
20. Gunter TE, Pfeiffer DR (1990) Mechanisms by which mitochondria transport calcium. *Am J Physiol* 258(5 Pt 1):C755–C786.
21. Schneider MD (2005) Cyclophilin D: Knocking on death's door. *Sci STKE* 2005(287): pe26.
22. Scheckhuber CQ, Wanger RA, Mignat CA, Osiewacz HD (2011) Unopposed mitochondrial fission leads to severe lifespan shortening. *Cell Cycle* 10(18):3105–3110.
23. Brust D, et al. (2010) Cyclophilin D links programmed cell death and organismal aging in *Podospora anserina*. *Aging Cell* 9(5):761–775.
24. Hamann A, Brust D, Osiewacz HD (2007) Deletion of putative apoptosis factors leads to lifespan extension in the fungal ageing model *Podospora anserina*. *Mol Microbiol* 65(4):948–958.
25. Toman J, Fiskum G (2011) Influence of aging on membrane permeability transition in brain mitochondria. *J Bioenerg Biomembr* 43(1):3–10.
26. Marchi S, et al. (2012) Mitochondria-Ros crosstalk in the control of cell death and aging. *J Signal Transduct* 2012:329635.
27. Osiewacz HD (2011) Mitochondrial quality control in aging and lifespan control of the fungal aging model *Podospora anserina*. *Biochem Soc Trans* 39(5):1488–1492.
28. Frey TG, Sun MG (2008) Correlated light and electron microscopy illuminates the role of mitochondrial inner membrane remodeling during apoptosis. *Biochim Biophys Acta* 1777(7–8):847–852.
29. Sun MG, et al. (2007) Correlated three-dimensional light and electron microscopy reveals transformation of mitochondria during apoptosis. *Nat Cell Biol* 9(9):1057–1065.
30. Scorrano L, et al. (2002) A distinct pathway remodels mitochondrial cristae and mobilizes cytochrome *c* during apoptosis. *Dev Cell* 2(1):55–67.
31. Perkins G, Bossy-Wetzel E, Ellisman MH (2009) New insights into mitochondrial structure during cell death. *Exp Neurol* 218(2):183–192.
32. Mootha VK, et al. (2001) A reversible component of mitochondrial respiratory dysfunction in apoptosis can be rescued by exogenous cytochrome *c*. *EMBO J* 20(4): 661–671.
33. Strauss M, Hofhaus G, Schröder RR, Kühlbrandt W (2008) Dimer ribbons of ATP synthase shape the inner mitochondrial membrane. *EMBO J* 27(7):1154–1160.
34. Bornhövd C, Vogel F, Neupert W, Reichert AS (2006) Mitochondrial membrane potential is dependent on the oligomeric state of F_1F_0-ATP synthase supracomplexes. *J Biol Chem* 281(20):13990–13998.
35. Baker LA, Watt IN, Runswick MJ, Walker JE, Rubinstein JL (2012) Arrangement of subunits in intact mammalian mitochondrial ATP synthase determined by cryo-EM. *Proc Natl Acad Sci USA* 109(29):11675–11680.
36. Giorgio V, et al. (2009) Cyclophilin D modulates mitochondrial F_0F_1-ATP synthase by interacting with the lateral stalk of the complex. *J Biol Chem* 284(49):33982–33988.
37. Soubannier V, et al. (2002) In the absence of the first membrane-spanning segment of subunit 4(b), the yeast ATP synthase is functional but does not dimerize or oligomerize. *J Biol Chem* 277(12):10739–10745.
38. Velours J, et al. (2011) Evidence of the proximity of ATP synthase subunits 6 (a) in the inner mitochondrial membrane and in the supramolecular forms of *Saccharomyces cerevisiae* ATP synthase. *J Biol Chem* 286(41):35477–35484.
39. Giorgio V, et al. (2013) Dimers of mitochondrial ATP synthase form the permeability transition pore. *Proc Natl Acad Sci USA* 110(15):5887–5892.
40. Weimann T, Vaillier J, Salin B, Velours J (2008) The intermembrane space loop of subunit b (4) is a major determinant of the stability of yeast oligomeric ATP synthases. *Biochemistry* 47(11):3556–3563.
41. Brenner C, Grimm S (2006) The permeability transition pore complex in cancer cell death. *Oncogene* 25(34):4744–4756.
42. van der Laan M, Bohnert M, Wiedemann N, Pfanner N (2012) Role of MINOS in mitochondrial membrane architecture and biogenesis. *Trends Cell Biol* 22(4):185–192.
43. Harner M, et al. (2011) The mitochondrial contact site complex, a determinant of mitochondrial architecture. *EMBO J* 30(21):4356–4370.
44. Hoppins S, et al. (2011) A mitochondrial-focused genetic interaction map reveals a scaffold-like complex required for inner membrane organization in mitochondria. *J Cell Biol* 195(2):323–340.
45. Kremer JR, Mastronarde DN, McIntosh JR (1996) Computer visualization of three-dimensional image data using IMOD. *J Struct Biol* 116(1):71–76.
46. Nicastro D, et al. (2006) The molecular architecture of axonemes revealed by cryoelectron tomography. *Science* 313(5789):944–948.
47. Pettersen EF, et al. (2004) UCSF Chimera—A visualization system for exploratory research and analysis. *J Comput Chem* 25(13):1605–1612.